Dirk Budelmann (Autor)

Electronic and Magnetic Properties of Pure and Structured Cuprate Superconductors. A Raman Scattering and Ellipsometry Study

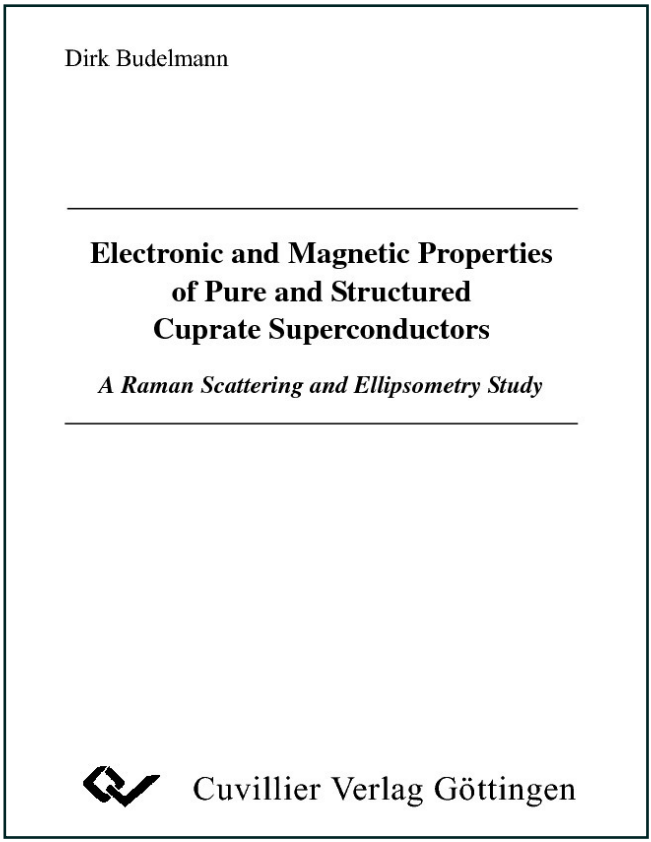

https://cuvillier.de/de/shop/publications/2962

Chapter 1

Introduction

This work is focused on the experimental investigation of one subclass of strongly correlated materials, the high-temperature superconductors. Since the discovery of superconducting mercury by H. Kamerlingh Onnes exhibiting a critical temperature T_c around 4 K, [1] new materials with higher T_c's have been found. The break-through was achieved by Bednorz and Müller in 1986,[2] when they reported the ceramic compound $La_{2-x}Ba_xCuO_4$ to enter the superconducting state around 35 K. This observation was the starting-point for a competition finding other compounds exhibiting higher T_c's. In 1987, Wu *et al.* synthesized $YBa_2Cu_3O_{7-\delta}$ with $T_c = 90$ K, i.e. above the boiling point of nitrogen.[3] Today, even a higher maximal T_c of 93.6 K was reported by Liang et al.[4] Some groups reported the synthesis of $HgBa_2Ca_2Cu_3O_{8+\delta}$ reaching a T_c higher than 164 K under high-pressure conditions.[5]

In this chapter, I present a short overview about the high-temperature superconductors that have been investigated. The basic fundamental treatment of light scattering in solid-state materials is introduced here also. A brief outline of the experimental setups for Raman scattering and spectroscopic ellipsometry is given in chapter 2. During the course of this work, our group invested serious efforts to setup the Ultimate Triple 3 Raman spectrometer.

In the following, applications of the Raman and ellipsometry technique are shown in chapters 3 and 4. First, we present data on the optical properties of pure films. Second, Raman data of two high-temperature superconducting single crystals for different excitation energies are shown. We use the Ultimate Triple and cover a spectral range from the visible to the ultraviolet. Third, we focus on superlattices with an overall thickness of about 300 nm. Superlattices consist of alternating layers of different materials. Here, we investigated superlattices composed of superconducting and antiferromagnetic insulating materials to study the interplay of antiferromagnetic and superconducting order parameters.

Some of the experiments described above have already been published or are submitted for publication. The papers are enumerated with roman numbers to simplify citations within this work. This thesis includes the following pre- and reprints:

I **Optical properties of $YBa_2Cu_3O_{7-\delta}$ and $PrBa_2Cu_3O_{7-\delta}$ films: High-energy correlations and metallicity**
J. Bäckström, D. Budelmann, R. Rauer, M. Rübhausen, H. Rodríguez, and H. Adrian
submitted

II **Proximity effect in $YBa_2Cu_3O_{7-y}$/$PrBa_2Cu_3O_{7-y}$ studied by inelastic light scattering**
D. Budelmann, S. Ostertun, M. Rübhausen, A. Bock, M. Schilling, H. Burkhardt, U. Merkt, and A. Krämer
Phys. Rev. B **63**, 174508 (2001)

III **Antiferromagnetic and superconducting proximity effects in $YBa_2Cu_3O_{7-\delta}$/$PrBa_2Cu_3O_{7-\delta}$ superlattices**
D. Budelmann, J. Holmlund, J. Andreasson, H. Rodríguez, J. Bäckström, L. Börjesson, H. Adrian, U. Merkt, and M. Rübhausen
Phys. Rev. B **67**, R140507 (2003)

Further contributions to the investigation of strongly correlated materials that are not directly related to this thesis are appended:

IV **Orbital ordering in $LaMnO_3$ investigated by resonance Raman spectroscopy**
R. Krüger, B. Schulz, S. Naler, R. Rauer, D. Budelmann, J. Bäckström, K.H. Kim, S-W. Cheong, V. Perebeinos, and M. Rübhausen
Phys. Rev. Lett. **92**, 097203 (2004)

V **Thickness dependent phase separation in $La_{0.7}Ca_{0.3}MnO_3$ films**
R. Rauer, J. Bäckström, D. Budelmann, M. Kurfiß, M. Schilling, M. Rübhausen, T. Walter, K. Dörr, and S.L. Cooper
Appl. Phys. Lett. **81**, 3777 (2002)

VI **Chiral excitations in the normal and superconducting states of $Bi_2Sr_2CaCu_2O_8$**
M. Rübhausen, R. Krüger, B. Schulz, D. Budelmann, J. Bäckström, M. V. Klein, P. Guptasarma, and D.G. Hinks
submitted

1.1 Cuprate Superconductors

From a theoretical point of view, the discovery of high-temperature superconductors raised an intense debate. While the theory of Bardeen, Cooper and Schrieffer (BCS) [6] allows to satisfactorily model the behavior of the conventional superconductors, it fails to describe the cuprates with their extraordinary high T_c's. In BCS theory, two charge carriers feel an attractive potential overpowering Coulomb repulsion due to the exchange of virtual phonons. This results in the formation of pairs, the so called Cooper pairs. For temperatures above 30 K the thermal fluctuations would disturb this pairing process. Hence, one has to consider the interplay between additional degrees of freedom that might support pair formation, of e.g. magnetic or electronic origin. The need to understand physics on the different energy scales makes it even more difficult to find an adequate theory. It still remains open if the interplay of the different degrees of freedom is of competitive or of constructive nature.[7]

Phase diagram

Cuprate superconductors have one or more CuO_2 (cuprate) layers in common. In first approximation, the charge carriers reside mainly within the cuprate planes and we find a quasi two-dimensional electron gas (2DEG). However, cuprates are rather much more complex and there are strong evidences for an important role of physics beyond the layers, e.g. the influence between the planes and the reservoirs.[8; 9]

The schematic phase diagram of cuprate superconductors is depicted in Fig. 1.1. Here, the cross-over temperatures versus effective hole doping p within the cuprate planes are plotted. For an underdoped cuprate, one finds a long-range three-dimensional antiferromagnetic phase (3D-AF) below the Néel temperature T_N. This phase corresponds to the half-filled Hubbard antiferromagnetic insulator, providing an upper and lower Hubbard band with a charge-transfer gap around 1.7 eV.[10] The antiferromagnetism is due to spin-$\frac{1}{2}$ charges residing at the Cu^{2+} sites within the cuprate planes. With increasing effective hole doping one observes a decreasing T_N. Short-range two-dimensional antiferromagnetic correlations (2D-AF) persist for an increased doping in the vicinity of the onset of superconducting properties. In the superconducting doping range we find a maximal T_c at optimal doping $p_{opt} = 0.16$ holes per cuprate plane and unit cell. For the overdoped samples with $p > p_{opt}$ one observes a decreasing T_c, and above T_c the compound shows the behavior of a "strange metal". Here, optical and transport studies exhibit an unconventional Fermi-liquid like behavior, e.g. the resistivity is following a T^2 law.[11] However, bandstruc-

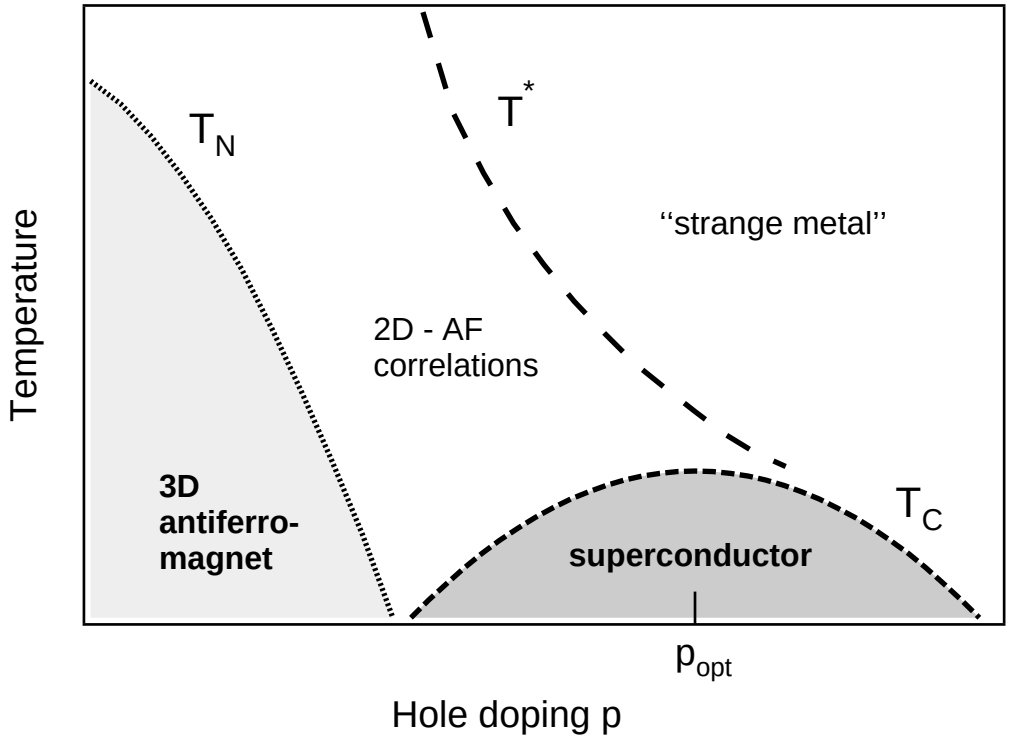

Figure 1.1: Generic phase diagram for the hole-doped cuprates.

ture calculations that apply the local density approximation (LDA) predict a metallic phase even for the undoped cuprates. This conflicting behavior is a signature of the strong electronic correlations in these compounds. In order to describe the cuprates, the Mott-Hubbard model seems to be promising. Here, the strong correlations are taken into account inducing a splitting to the lower and the upper Hubbard band.[12]

Between the "strange metal" and the 2D-AF phase we find the pseudogap temperature T^*. The nature of the pseudogap is still under debate and will not be discussed here in any depth. One explanation of the pseudogap is a precursor effect of the superconducting state where the pair formation is incoherent and fluctuating.[13] But it is still not clear if the pseudogap is either a pre-phase of superconductivity, a competing state or completely independent of superconductivity.[14] Pseudogap effects can be observed by many experiments in the underdoped cuprates.[15] The formation of a pseudogap is predicted in terms of the doped Mott-Hubbard insulator theory when strong local correlations are included ("Mottness").[12]

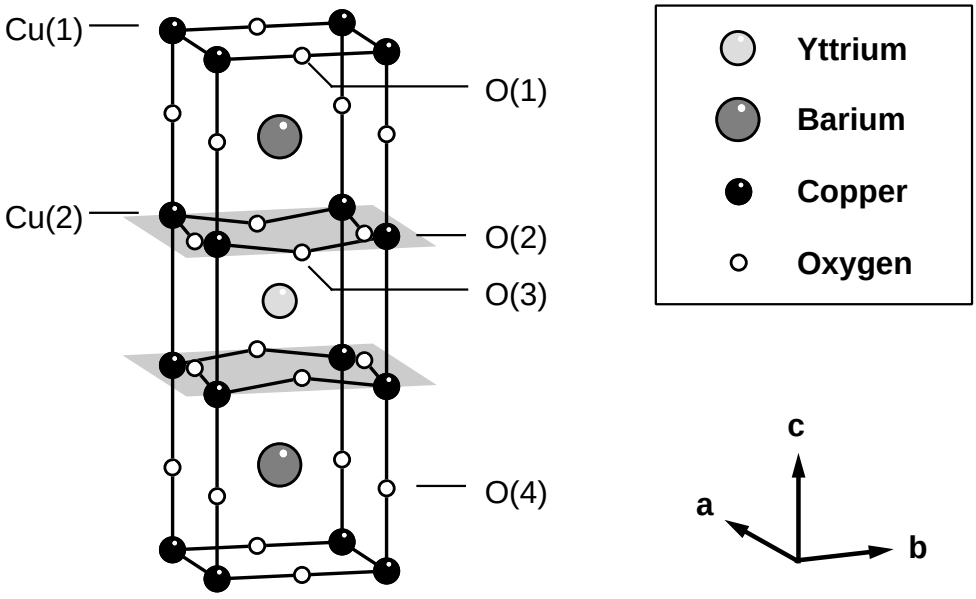

Figure 1.2: Orthorhombic unit cell for the $YBa_2Cu_3O_7$ compounds. The space group is *Pmmm*. Cuprate planes are indicated by the gray areas.

$YBa_2Cu_3O_7$ compounds

Figure 1.2 shows the orthorhombic unit cell of the family $YBa_2Cu_3O_7$ (Y-123), where the central atom Y can be substituted by most rare-earth atoms without changing superconducting properties essentially. One exception is the well studied substitution of Y by Pr in the $Y_{1-x}Pr_xBa_2Cu_3O_7$ compounds. With increasing x one can reduce the effective hole doping p within the cuprate planes. One observes a decreasing T_c until it vanishes completely around $x \geq 0.55$.[16] On the other hand, antiferromagnetic domain sizes are growing with increasing Pr doping what has been intensively studied by Raman spectroscopy.[17; 18]

The single copper-oxide chains (CuO) running in *b*-direction have been attributed to perform as charge reservoirs for the planes. When one deoxygenates $YBa_2Cu_3O_{7-\delta}$ by removing oxygen from the chains, the effective hole doping within the planes decreases. The oxygen content δ varies between 0 and 1. However, one finds the optimal doping for Y-123 with a T_c around 93.6 K for $\delta = 0.05$.[4] The undoped $YBa_2Cu_3O_6$ compound is an antiferromagnetic insulator exhibiting a high Néel temperature above 500 K.[19]

Both doping methods lead to a structural change of the unit cell. While Y-substitution alters lattice parameters and inter-atomic distances due to different ionic sizes of the rare earths, we find tetragonal structure for fully deoxygenated insulating compounds. An orthorhombic distortion appears for increasing δ and